Journal Name

COMMUNICATION

Guest control of a hydrogen bond-catalysed molecular rotor

Gregory T. Rushton,[a] Erik C. Vik[a], William G. Burns,[a] Roger D. Rasberry,[a] and Ken D. Shimizu[a]*

Received 00th January 20xx,
Accepted 00th January 20xx

DOI: 10.1039/x0xx00000x

www.rsc.org/

Demonstrated is the control of a molecular rotor using hydrogen bonding guests. With a properly positioned phenol substituent, the *N*-arylimide rotors can form an intramolecular hydrogen bond that catalyses the rotational isomerization process. The addition of guests disrupts the hydrogen bond and raises the rotational barrier slowing rotation by two orders of magnitude.

The design and development of molecular machines provide exciting new frontiers in synthetic chemistry.[1–4] Some of the most common types are molecular rotors, motors, and brakes.[5–8] Three general strategies have been employed to control the rates of rotation and rotational barriers of molecular devices. These include modulating sterics,[9–12] bond order,[13,14] and intramolecular hydrogen bonding interactions of the systems.[15–19] This last category allows control of the molecular rotors and molecular brakes using hydrogen bonding guests. In most cases, the intramolecular hydrogen bond slows the rate of rotation, and thus, the addition of a hydrogen bonding guest that can disrupt the intramolecular hydrogen bond increases the rate of rotation.[15,20] Presented is a molecular rotor that slows by four orders of magnitude upon addition of a hydrogen bonding guest via a unique mechanism of disrupting an intramolecular hydrogen bond that catalyses the bond rotation. In the absence of guest, the molecular brake forms the intramolecular hydrogen bond in the transition state that facilitates and catalyses bond rotation.[16–18] In the course of developing molecular devices based on the atropisomeric *N,N'*-diaryl naphthalenediimides, we observed that diol **1** had an unexpectedly low rotational barrier.[19–32] This atropisomeric framework forms distinct *syn*- and *anti*-rotamers due to restricted rotation of the *N*-aryl rotors. Usually, the rotamers are stable at room temperature with rotational barriers above 27 kcal/mol. For example, diether **2** has a rotational barrier of 27.5 kcal/mol and the rotamers can be separated at room temperature using column chromatography.[32] In contrast, diol **1** has a significantly lower rotational barrier of 21.3 kcal/mol and rotates over 10,000 times faster than diether **2**.

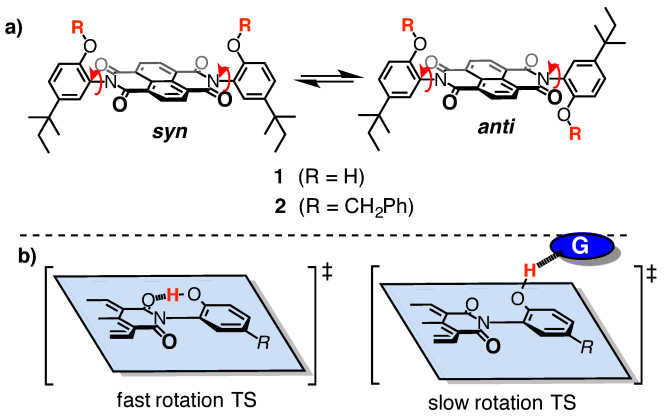

Fig. 1 (a) The *syn-anti* conformational equilibrium for *N,N'*-diarylnaphthalene diimide rotamers **1** and **2**; and (b) the transitions states for bond rotation in diol **1** (left) and diol **1** with a hydrogen bonded guest (right).

Initially, we attributed the difference in rotational barriers to the larger steric presence of the OCH_2Ph groups in diether **2** versus the OH groups in diol **1**. However, modelling and crystallographic studies found that phenol and benzyl ether substituents have similar steric profiles because the CH_2Ph and H groups on the oxygens point away from the central naphthalene diimide spacer (Fig. 1a).[32] Thus, an alternate explanation was examined in which the acidic proton of the phenol formed an intramolecular hydrogen bond (Fig. 1b) that stabilized the planar transition state and lowered the rotational barrier of diol **1**. A similar intramolecular hydrogen bond hypothesis was proposed by Roussel to explain the 5 kcal/mol lower rotational barriers of *N*-aryl rotors **A** and **B** with *ortho*-OH groups (Table 1) in comparison to the analogous

[a] *Department of Chemistry and Biochemistry, University of South Carolina, Columbia, SC 29208 USA.*

† Footnotes relating to the title and/or authors should appear here.
Electronic Supplementary Information (ESI) available: [details of any supplementary information available should be included here]. See DOI: 10.1039/x0xx00000x

rotors with *ortho*-OR groups.[16,17] Another example is our *N*-arylimide molecular brake in which an intramolecular hydrogen bond in the transition state acts as 'proton grease' lowering the rotational barrier by 9.3 kcal/mol.[19]

Table 1 Literature examples of similar *N*-aryl rotors with lower rotational barriers for phenol (R = H) versus ether (R = CH_3) derivatives.[16,17]

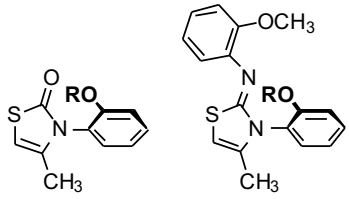

	A	B
	$\Delta G^{\ddagger}$	$\Delta G^{\ddagger}$
R = H	20.9 kcal/mol	21.0 kcal/mol
R = CH_3	26.4 kcal/mol	25.6 kcal/mol

First, the rotational barriers of diol **1** and diether **2** were computationally modelled to verify the presence and influence of an intramolecular hydrogen bond in the planar transition state. The DFT method M06-2X/6-31G* was selected as it provides a good balance of accurate steric and hydrogen bonding energies. The symmetry of the atropisomeric *N,N*-diimide platforms enabled analysis of a substructure containing a single *N*-arylimide rotor (Fig. 2), which greatly shortened calculation times. A dihedral angle driver was used to systematically calculate the energy of structures along the rotational barrier energy surface (Fig. 3) and the GS and TS structures were identified. The calculated rotational barriers of the phenol and benzyl ether (18.6 and 26.4 kcal/mol) rotors were very similar to the experimental values (21.3 and 27.5 kcal/mol). More importantly, the computational studies were able to replicate the significantly lower rotational barrier of the phenol rotor.

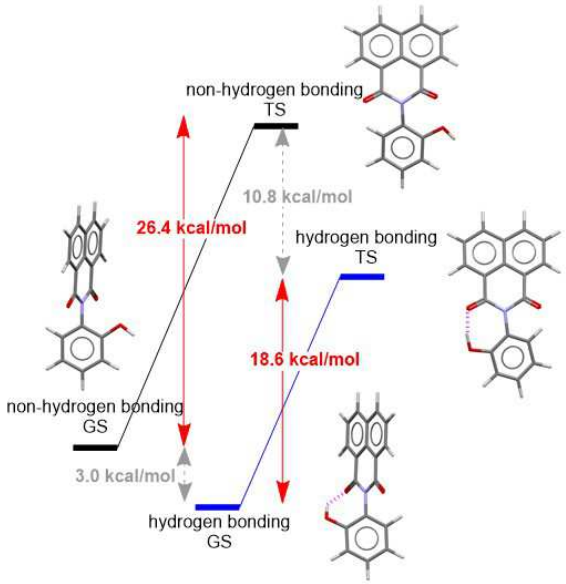

Fig. 2 Calculated GS and TS structures (M06-2X/6-31G*) and barrier heights for the phenol *N*-arylimide rotors allowed to form (blue lines) or constrained to prevent (black lines) the formation of intramolecular hydrogen bonds.

The computational studies also enabled examination of the role of intramolecular hydrogen bonding on the rotational barrier. In support of our hypothesis, a strong well-defined hydrogen bond was formed in the transition state (Fig. 2) as evidenced by an extremely short =O-to-H distance (1.557 Å). For comparison, the barrier was also calculated for a geometry in which the OH group was constrained (Fig. 2, black lines) to point away from the imide carbonyl and was unable to form an intramolecular hydrogen bond. The barrier for the non-hydrogen bonding phenol rotor was much higher (26.4 kcal/mol) in comparison to the unconstrained hydrogen bonding phenol rotor (18.6 kcal/mol). The higher barrier of the non-hydrogen bonding geometry was very similar to the benzyl ether rotor (26.4 kcal/mol) confirming that the phenol and ether substituents have similar steric effects on the TS in the absence of a hydrogen bond. This confirmed that the differences in rotational barriers between diol **1** and diether **2** were primarily due to the ability of diol **1** to form an intramolecular hydrogen bond.

Interestingly, the phenol rotor could also form an intramolecular hydrogen bond that stabilized the ground state (Fig. 2). However, this GS hydrogen bond was much weaker than the TS hydrogen bond as was evident from its greater length (1.856 Å) and non-linear geometry (144°). Corroboration was provided by a comparison of the ground states and transition states for the constrained and unconstrained systems (Fig. 2, grey arrows). The GS hydrogen bond was 3.0 kcal/mol; whereas the TS hydrogen bond was 10.8 kcal/mol.

The addition of various hydrogen bonding guests, provided a unique means to control the rotational barrier of diol **1** and also verified the importance of the TS hydrogen bond. Small molecule guests were used as opposed to changing the bulk solvent to minimize variations in solvent polarity or viscosity. The guests compete for and disrupt the intramolecular hydrogen bond raising the rotational barrier, as shown in Fig. 1b. Small molecule hydrogen bonding guests were selected with varying hydrogen bond accepting abilities: acetic acid, acetone, THF, pyridine, triethylamine (TEA), and DMSO.

The rates of rotation were measured by monitoring the *syn/anti* ratio of *anti*-enriched samples of diol **1** and diether **2** as they approached equilibrium in solution at 18.2 °C and 70.1 °C, respectively. *Anti*-enriched samples of diol **1** were prepared by crystallization.[32] *Anti*-enriched samples of diether **2** were prepared by treating the *anti*-enriched diol **1** with benzyl chloride and potassium carbonate in dry DMF at 0 °C.[32] All of the measurements were carried out in a solvent (72:28 (v/v), benzene-d6:acetonitrile-d3) that would not disrupt the hydrogen bonding interactions, while yielding distinct peaks in the ^{1}H NMR spectra for the *syn*- and *anti*-conformers of diol **1** and diether **2**.

In each case, the addition of the hydrogen bonding guests (200 equivalents) increased the rotational barrier of diol **1** (Fig.

3). By comparison, the rotational barrier for diether **2** did not change significantly on addition of 200 equivalents of the same hydrogen bonding guests. The sharp contrast in the sensitivities of diol **1** and diether **2** to the addition of hydrogen bonding guests were consistent with the proposed mechanisms. For diol **1**, the hydrogen bonding guests disrupted the TS stabilising intramolecular hydrogen bond raising the rotational barrier. For diether **2**, the hydrogen bonding guests have little or no effect on the rotational barrier as diether **2** cannot form an intramolecular hydrogen bond.

Quantitative analysis of the effects of each guest provided additional support for the role of the intramolecular hydrogen bond in diol **1**. The measured rotational barriers in the presence of each guest were plotted against the hydrogen bond accepting ability of the guest, as measured by the Kamlet-Taft β parameter (Fig. 3). An excellent linear correlation was observed between the rotational barriers of diol **1** and the β parameters of the guests. DMSO, which was the strongest hydrogen bond acceptor in the series, showed the most dramatic effect raising the barrier of diol **1** by 2.3 kcal/mol. Weaker hydrogen bond acceptors such as acetic acid, THF, and acetone had much smaller effects raising barrier by only 0.6-0.7 kcal/mol.

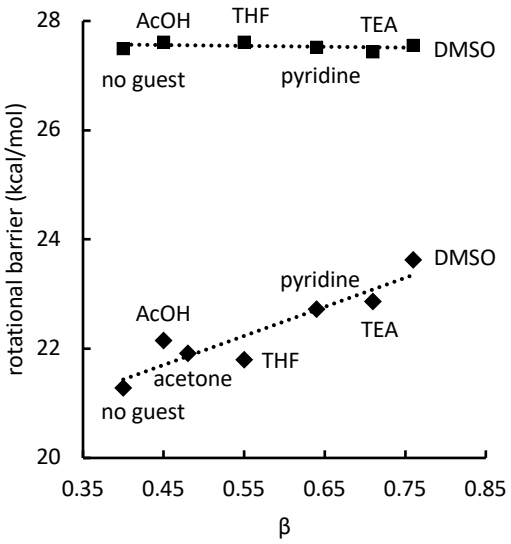

Fig. 3 Correlation of the measured rotational barriers of diol **1** (diamonds) and diether **2** (squares) in the presence of 200 eq of guests against the Kamlet-Taft hydrogen bond accepting parameter (β) of the guests. The rotational barriers were measured in 72:28 (v/v) benzene-d6:acetonitrile-d3 at 18.2 and 70.1 °C, respectively. The error in the measurements were within the data markers. Acetone was not tested against diether **2** because its boiling point is lower than 70.1 °C. The points labelled no guest were assigned the β of acetonitrile.

To test the possibility that the guests were raising the rotational barriers of **1** by hydrogen bonding to and stabilising the ground state, ^{1}H NMR titration studies were conducted. The measured association constants of DMSO and acetone for diol **1** in benzene-acetonitrile (72:28, v/v) were 8.9 x 10^{-1} and 1.0 x 10^{-2} M^{-1}, respectively. These association constants are very low (K_a < 1). Thus, the stabilization of the ground states by the guests is small or negligible and could not explain the dramatic changes in the rotational barriers in the presence of these guests.

The dynamic hydrogen bonding interactions of the guests enabled the reversible turning ON and OFF of the braking effect. For this demonstration, CD_2Cl_2 was selected as the solvent system so that the polar hydrogen bonding guest (DMSO) could be removed by aqueous extraction. The rate of rotation of a solution of *anti*-enriched **1** in CD_2Cl_2 was measured for two complete ON-OFF cycles by adding and removing DMSO (Fig. 4). Due to the rapid isomerization of diol **1** in the absence of guest, this study was started with the brake engaged (with DMSO) and the temperature was kept at -10 °C for the entire experiment. The rate of rotation sped up and slowed down by two orders of magnitude with the removal and then addition of DMSO. After two cycles, the diol reached the *syn/anti* equilibrium ratio, and the rate of interconversion could no longer be observed.

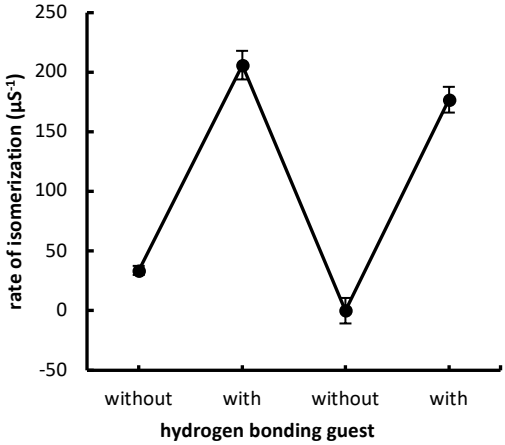

Fig. 4 Measured rate constants for a single sample of diol **1** in CD_2Cl_2 in the presence (with) and absence (without) 5 eq. of DMSO for two complete cycles.

In conclusion, the rotational barrier of a *N,N*'-diarylnaphthalenediimide molecular rotor can be tuned using guests with different hydrogen bonding abilities. The key to this system is the presence of an intramolecular hydrogen bond in the transition state that catalyses bond rotation. The guests disrupt the intramolecular hydrogen bond, raising the rotational barrier. The magnitude of the rate acceleration could be modulated by the hydrogen bond accepting ability and number of equivalents of the hydrogen bonding guest. In future work, we aim to use this rotor as an enzyme model system to study the role of transition state stabilization by hydrogen bonding.

Acknowledgements

This work was supported by NSF grants CHE 1310139 and 1709086.

Notes and references

1 V. Balzani, A. Credi, F. M. Raymo and J. F. Stoddart, *Angew. Chem. Int. Ed.*, 2000, **39**, 3348–3391.
2 E. R. Kay, D. A. Leigh and F. Zerbetto, *Angew. Chem. Int. Ed.*, 2007, **46**, 72–191.
3 S. Erbas-Cakmak, D. A. Leigh, C. T. McTernan and A. L. Nussbaumer, *Chem. Rev.*, 2015, **115**, 10081–10206.
4 A. Coskun, M. Banaszak, R. D. Astumian, J. F. Stoddart and B. A. Grzybowski, *Chem. Soc. Rev.*, 2011, **41**, 19–30.
5 G. S. Kottas, L. I. Clarke, D. Horinek and J. Michl, *Chem. Rev.*, 2005, **105**, 1281–1376.
6 T.-A. V. Khuong, J. E. Nuñez, C. E. Godinez and M. A. Garcia-Garibay, *Acc. Chem. Res.*, 2006, **39**, 413–422.
7 K. Skopek, M. C. Hershberger and J. A. Gladysz, *Coord. Chem. Rev.*, 2007, **251**, 1723–1733.
8 A. Comotti, S. Bracco and P. Sozzani, *Acc. Chem. Res.*, 2016, **49**, 1701–1710.
9 T. R. Kelly, M. C. Bowyer, K. V. Bhaskar, D. Bebbington, A. Garcia, F. Lang, M. H. Kim and M. P. Jette, *J. Am. Chem. Soc.*, 1994, **116**, 3657–3658.
10 J. Rebek, T. Costello, L. Marshall, R. Wattley, R. C. Gadwood and K. Onan, *J. Am. Chem. Soc.*, 1985, **107**, 7481–7487.
11 P. V. Jog, R. E. Brown and D. K. Bates, *J. Org. Chem.*, 2003, **68**, 8240–8243.
12 Jye-Shane Yang, Yao-Ting Huang, Jinn-Hsuan Ho, Wei-Ting Sun, Hsin-Hau Huang, Ying-Chih Lin, Shing-Jong Huang, Shou-Ling Huang and Hsiu-Feng Lu, *Org. Lett.*, 2008, **10**, 2279–2282.
13 Cheng-Hua Yang, Ch. Prabhakar, Shou-Ling Huang, Ying-Chih Lin, Wei Shyang Tan, Nimesh C. Misra and Wei-Ting Sun, *Org. Lett.*, 2011, **13**, 5632–5635.
14 M. C. Basheer, Y. Oka, M. Mathews and N. Tamaoki, *Chem. – Eur. J.*, 2010, **16**, 3489–3496.
15 Ignacio Alfonso, M. Isabel Burguete and Santiago V. Luis, *J. Org. Chem.*, 2006, **71**, 2242–2250.
16 N. Vanthuyne, F. Andreoli, S. Fernandez, M. Roman and C. Roussel, *Lett. Org. Chem.*, 2005, **2**, 433–443.
17 C. Roussel, N. Vanthuyne, M. Bouchekara, A. Djafri, J. Elguero and I. Alkorta, *J. Org. Chem.*, 2008, **73**, 403–411.
18 Y. Aydeniz, F. Oğuz, A. Yaman, A. S. Konuklar, I. Doğan, V. Aviyente and R. A. Klein, *Org. Biomol. Chem.*, 2004, **2**, 2426–2436.
19 B. E. Dial, P. J. Pellechia, M. D. Smith and K. D. Shimizu, *J. Am. Chem. Soc.*, 2012, **134**, 3675–3678.
20 B. E. Dial, R. D. Rasberry, B. N. Bullock, M. D. Smith, P. J. Pellechia, S. Profeta and K. D. Shimizu, *Org. Lett.*, 2011, **13**, 244–247.
21 E. Kumarasamy, R. Raghunathan, M. P. Sibi and J. Sivaguru, *Chem. Rev.*, 2015, **115**, 11239–11300.
22 K. Kishikawa, K. Yoshizaki, S. Kohmoto, M. Yamamoto, K. Yamaguchi and K. Yamada, *J. Chem. Soc. Perkin 1*, 1997, 1233–1240.
23 K. Kishikawa, C. Iwashima, S. Kohmoto, K. Yamaguchi and M. Yamamoto, *J. Chem. Soc. Perkin 1*, 2000, 2217–2221.
24 R. D. Rasberry and K. D. Shimizu, *Org. Biomol. Chem.*, 2009, **7**, 3899–3905.
25 P. Li, C. Zhao, M. D. Smith and K. D. Shimizu, *J. Org. Chem.*, 2013, **78**, 5303–5313.
26 J. Hwang, P. Li, W. R. Carroll, M. D. Smith, P. J. Pellechia and K. D. Shimizu, *J. Am. Chem. Soc.*, 2014, **136**, 14060–14067.
27 J. M. Maier, P. Li, J. Hwang, M. D. Smith and K. D. Shimizu, *J. Am. Chem. Soc.*, 2015, **137**, 8014–8017.
28 P. Li, J. Hwang, J. M. Maier, C. Zhao, D. V. Kaborda, M. D. Smith, P. J. Pellechia and K. D. Shimizu, *Cryst. Growth Des.*, 2015, **15**, 3561–3564.
29 J. Hwang, P. Li, M. D. Smith and K. D. Shimizu, *Angew. Chem. Int. Ed.*, 2016, **55**, 8086–8089.
30 Y. Zhang, J. M. Lavin and K. D. Shimizu, *J. Am. Chem. Soc.*, 2009, **131**, 12062–12063.
31 Y. S. Chong, M. D. Smith and K. D. Shimizu, *J. Am. Chem. Soc.*, 2001, **123**, 7463–7464.
32 Y. S. Chong, B. E. Dial, W. G. Burns and K. D. Shimizu, *Chem. Commun.*, 2012, **48**, 1296–1298.

